Terahertz Plasmonic Quantum Cascade Lasers: A Comprehensive Physics Study

Faezeh Pakfetrat
Shiraz University of Technology
Hassan Pakarzadeh (pakarzadeh@sutech.ac.ir)
Shiraz University of Technology https://orcid.org/0000-0002-7561-4088

Research Article

Keywords: Terahertz, quantum cascade laser, plasmonics, rate equations, gain spectrum, antenna feedback.

Posted Date: October 25th, 2021

DOI: https://doi.org/10.21203/rs.3.rs-993272/v1

Version of Record: A version of this preprint was published at Plasmonics on January 12th, 2022. See the published version at https://doi.org/10.1007/s11468-021-01584-6.

Terahertz Plasmonic Quantum Cascade Lasers: A Comprehensive Physics Study

Faezeh Pakfetrat and Hassan Pakarzadeh*
Department of Physics, Shiraz University of Technology, Shiraz, Iran
Corresponding author's e-mail: pakarzadeh@sutech.ac.ir

Abstract: Generation of terahertz (THz) radiation has been a hot research topic in recent years. Plasmonic quantum cascade lasers (QCLs) are among the most compact and efficient sources to generate THz radiation. In this paper, we comprehensively study plasmonic QCLs designed based on the antenna-feedback structure to generate efficient radiation about the center frequency of 3 THz. By changing the geometric structure of the plasmonic cavity and using two-dimensional simulation, a minimum loss less than 5.9 cm^{-1} is achieved at the lasing frequency. It is also possible to control the orientation of the output beam either vertically or tilted by changing the geometry of the antenna design via chirped or non-chirped grating scheme. Moreover, the output characteristics of the QCL are simulated based on the three-level rate equations through which the dynamics of the laser, as well as the *P-I* curve are investigated. Also, the gain spectra for two laser designs (with chirped and non-chirped gratings) are simulated and compared to each other. The results of this paper may provide deep insight into designing efficient laser sources in the THz region.

Keywords: Terahertz; quantum cascade laser; plasmonics; rate equations; gain spectrum; antenna feedback.

1- Introduction

Terahertz (THz) sources have attracted specific attention for generating efficient radiation in the THz region [1]. THz radiation or T-ray includes a frequency range of 0.1-10 THz and an equivalent wavelength region of 30μm-3mm in the electromagnetic spectrum [2]. Many solids and molecules have distinct and strong spectral lines at THz frequencies that provide THz technology for both scientific and commercial applications in various fields such as biomedical imaging, non-invasive inspections, spectroscopy, and astronomy [3-7]. The generation of THz radiation is possible through various sources such as parametric oscillators [8], Gyrotrons [9, 10], and four-wave mixing (FWM) [11] which unfortunately generate low average power.

Quantum cascade lasers (QCLs) are one of the best available solid-state sources for generating high-average coherent THz radiation [12, 13]. QCLs operate based on intersubband transitions where the unipolar nature of the intersubband transitions creates the possibility of cascading process. QCLs can be fabricated using grating outside the cavity with the active region made of GaAs / AlGaAs [14]. The cooling system of these structures is based on liquid nitrogen with the operating temperature of 78° K [15, 16]. Metal-metal plasmonic waveguides with parallel plates are the most effective technique to confine THz radiation of QCLs due to the low optical loss of metals at this frequency range [17].

In this paper, antenna-feedback QCLs are comprehensively studied, and using the two-dimensional simulation, the lasing frequency and the intensity pattern are determined. The output characteristics of THz QCLs such as output power and optical gain are simulated using three-level rate equations. Also, the effect of injection current on the population inversion and the number of photons is examined where the P-I diagram and the optical gain spectrum of THz QCLs are plotted for two different types of feedback schemes, i.e., chipped and the non-chirped gratings. The results show that for the QCL with non-chirped grating scheme, a lower threshold current and higher slope efficiency are obtained. We believe that this is the first time that all aspects of such antenna-feedback THz QCLs are comprehensively studied all in one place.

2- Theoretical Framework

The schematic of the THz plasmonic QCL with the antenna-feedback grating on the top-metal cladding with a periodicity of Λ is shown in Fig. 1. The lateral and longitudinal absorbing boundaries are implemented to selectively excite the desired fundamental mode. It is worth noting that this THz QCL has been fabricated where its scanning electron microscope (SEM) image has been reported in ref. [14]. Also, by adjusting the grating period (Λ=21.7 μm), the laser will be surface-emitting with the grating period being obtained via [14]:

$$\lambda = \frac{\left(n_a + n_s\right)\Lambda}{p} \tag{1}$$

In Eq. (1), the refractive indices of the active medium and surrounding media (air) are $n_a \sim 3.6$ and $n_s=1$, respectively and the diffraction order is $p=1$ for the antenna- feedback design [14].

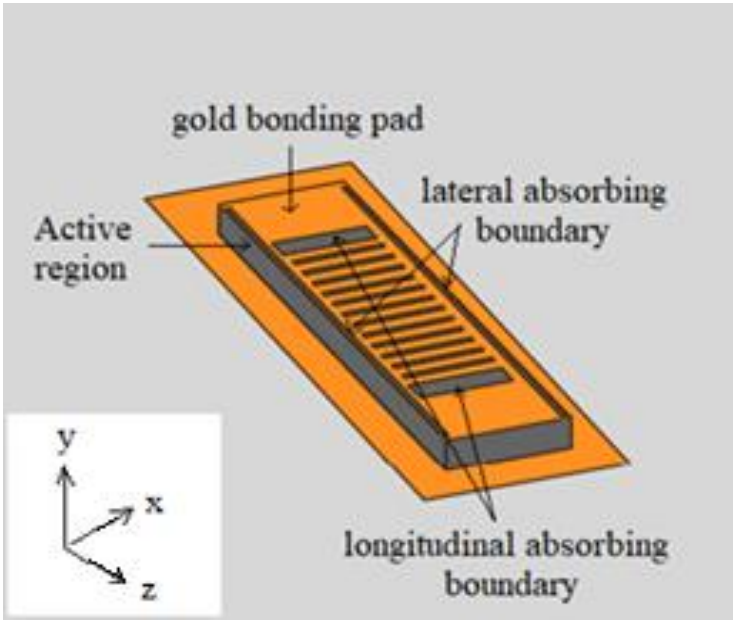

Fig 1. Schematic of the THz plasmonic QCL with the antenna-feedback grating implemented on the top-metal cladding with a periodicity of Λ [14].

The performance of the THz QCLs can be accurately described using several different numerical methods, such as the model of self-consistent rate equations [18]. Fig. 2 shows a schematic of the three-level electronic diagram of the QCLs. Stimulated emission is possible by population inversion between laser levels of 3 and 2 [19].

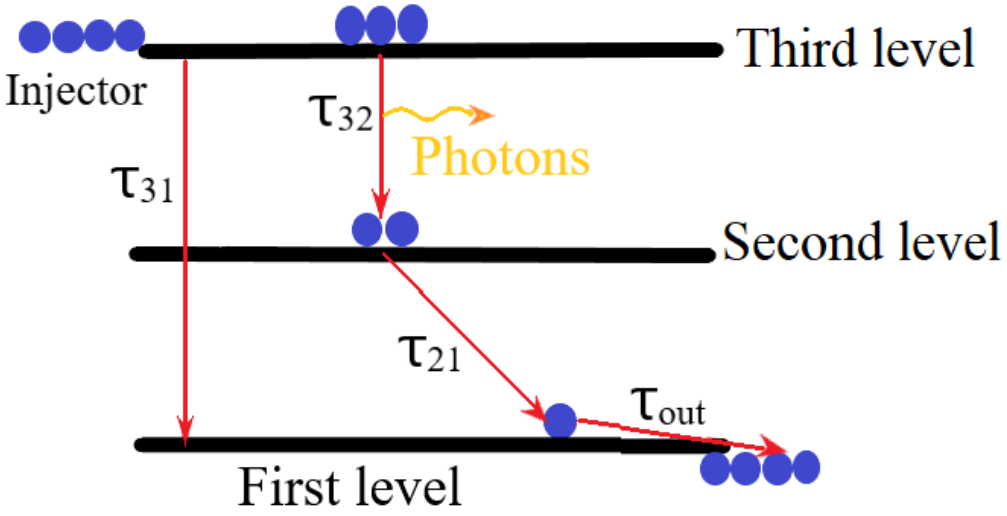

Fig 2. Assignment of three electronic levels for QCLs [19].

The output and dynamic characteristics of the QCL can be described by the following three-level rate equations [19] where the equations can be solved numerically using MATLAB software:

$$\frac{dN_3}{dt} = \eta \frac{I}{q} - \frac{N_3}{\tau_{32}} - \frac{N_3}{\tau_{31}} - g_0 S \Delta N \tag{2}$$

$$\frac{dN_2}{dt} = \frac{N_3}{\tau_{32}} - \frac{N_2}{\tau_{21}} + g_0 S \Delta N \tag{3}$$

$$\frac{dN_1}{dt} = \frac{N_3}{\tau_{31}} + \frac{N_2}{\tau_{21}} - \frac{N_1}{\tau_{out}} \tag{4}$$

$$\frac{dS}{dt} = \left[m g_0 \Delta N - \frac{1}{\tau_p} \right] S + m\beta \frac{N_3}{\tau_{sp}} \tag{5}$$

Here, η is the injection efficiency, I is the injection current, q is the electric charge, N_1, N_2, N_3 are the carrier populations in levels 1, 2 and 3, respectively. $\Delta N = N_3 - N_2$ is the population inversion, g_0 is the gain coefficient and S determines the number of cavity photons. τ_{32}, τ_{31} and τ_{21} are the lifetime representing the transition between the corresponding levels, τ_{out} denotes the tunnelling rate, τ_{sp} is the spontaneous emission lifetime, τ_p is the photon lifetime, m represents the multiplication factor and β is the spontaneous emission coupling coefficient [19].

The output power and optical gain of the THz QCL can be calculated using rate equations where the effect of various parameters such as frequency, refractive index and population inversion can be investigated. The output power of the laser is obtained via the equation [16]:

$$P = \frac{\pi c h \omega_0}{4nL\pi} \left(\frac{\alpha_{mir}}{\alpha_{cav}} \right) S \tag{6}$$

where L is the length of the laser cavity, $\hbar$ is the reduced Planck constant, c is the speed of light, n is the effective refractive index of the laser, α_{mir} is the cavity facet loss and α_{cav} is the cavity radiative loss. The optical gain of the laser is obtained from [20]:

$$g(f) = \Delta N \frac{q^2 \pi L^2 |d|^2 f_0}{\hbar n c \varepsilon_0} L(f) \tag{7}$$

where f_0 denotes resonance frequency, $|d|^2$ is the dipole matrix element where its value for GaAs is equal to 5.6 Å, and $L(f)$ is the Lorentz line shape function.

3- Results and Discussion

Using the finite-element method and physics of wave optics in the frequency domain, we have simulated the metal-metal parallel plate waveguide with GaAs/ AlGaAs active region. By adjusting different parameters in two dimensions with appropriate mesh grid, the loss spectrum is simulated to obtain the lasing frequency with the minimum resonance loss. A very important parameter for finite-element simulation is the mesh size. The mesh size should be accurate enough compared with the geometry size of the structure. On the other hand, the mesh size should be in consistence with the computational memory and simulation time [14].

Two highly doped layers of GaAs are placed at both ends of the active region as adsorbing boundaries with different widths. The gap size between the gold gratings is 0.2Λ, the width of the absorbing boundaries is 10 μm and its thickness is 0.1 μm. The length of the cavity is 1.4 mm, its thickness is 10 μm and the thickness of the gold layer is 0.4 μm (see Fig. 1).

We examine the laser loss at different frequencies as shown in Fig. 3 (a). The minimum loss of the resonance frequency occurs at 3.12 THz. Also, the laser output intensity pattern along the entire length of the cavity shown in Fig. 3 (b) where the maximum intensity takes place in the middle of cavity with vertical orientation.

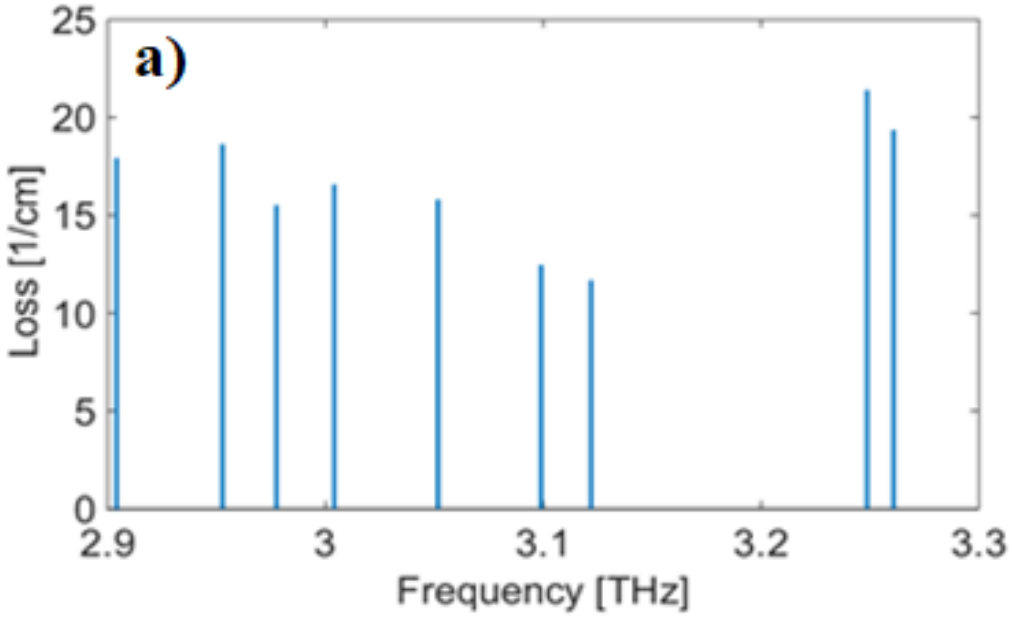

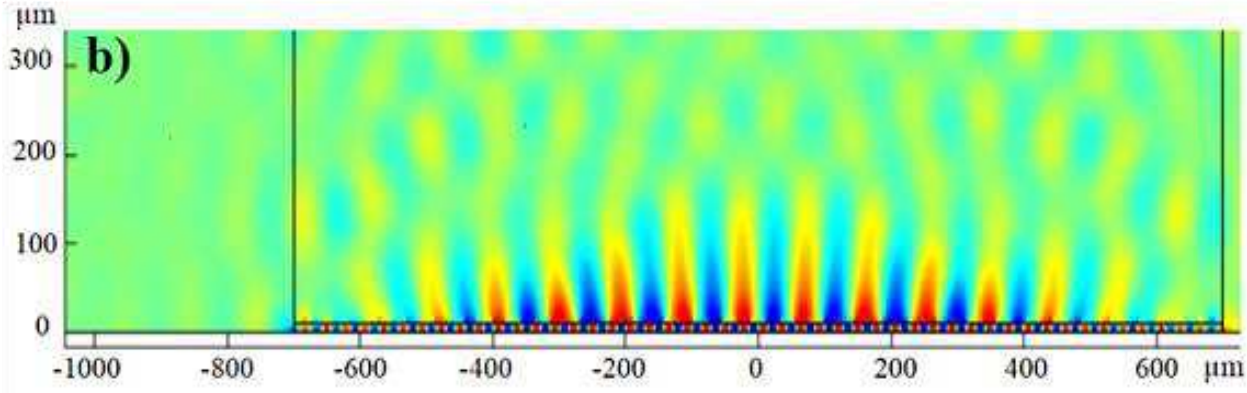

Fig 3. a) The loss spectrum for the antenna-feedback THz QCL with 21.7µm grating period where the minimum loss at 3.12 THz resonance frequency is about 12 cm^{-1}; b) The laser output intensity pattern along the entire length of the cavity.

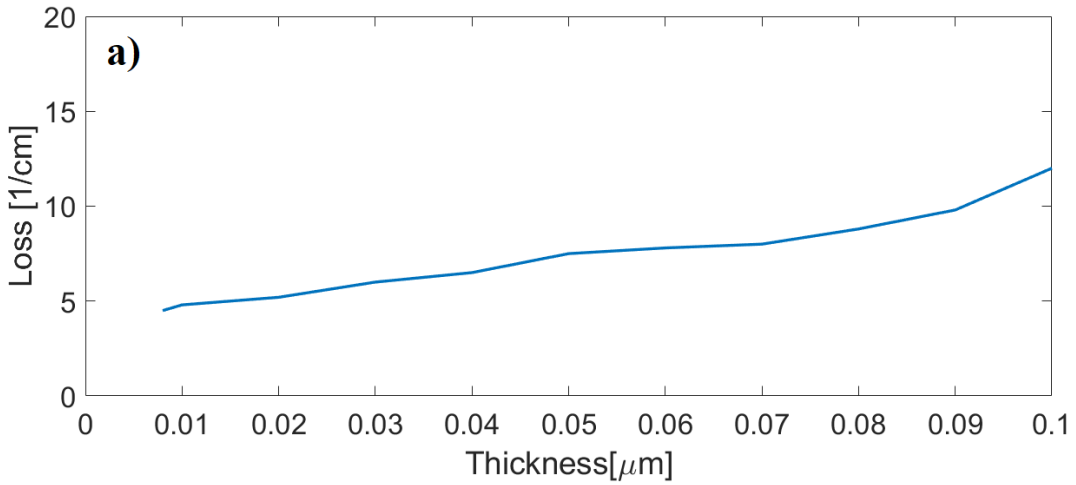

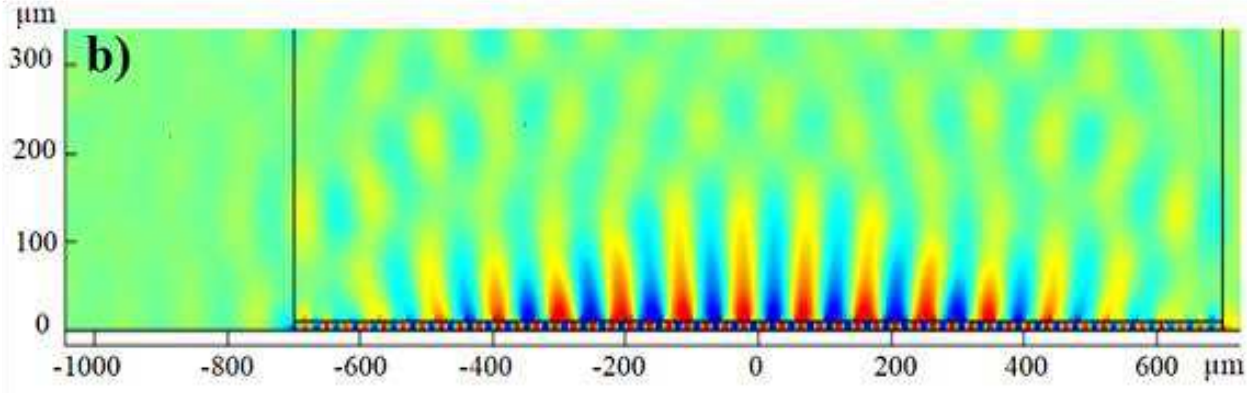

Fig 4. a) Laser frequency loss as a function of the thickness of the absorbing boundaries; b) laser output intensity pattern simulated at absorbing boundaries with the thickness of 0.008µm.

As shown in Fig. 4 (a), when the thickness of the absorbing boundaries increases, the laser loss increases as well. Fig. 4 (b) shows the laser output intensity pattern when the thickness of the absorbing boundaries is 0.008µm and the intensity height (approximately 135µm above the surface) is increased. It is found that by increasing the thickness of the metal grating to 1µm with the grating period of Λ=21µm and the thickness of the absorbing boundaries 0.05µm, a resonant loss of 5.91cm^{-1} can be achieved at 3.12THz.

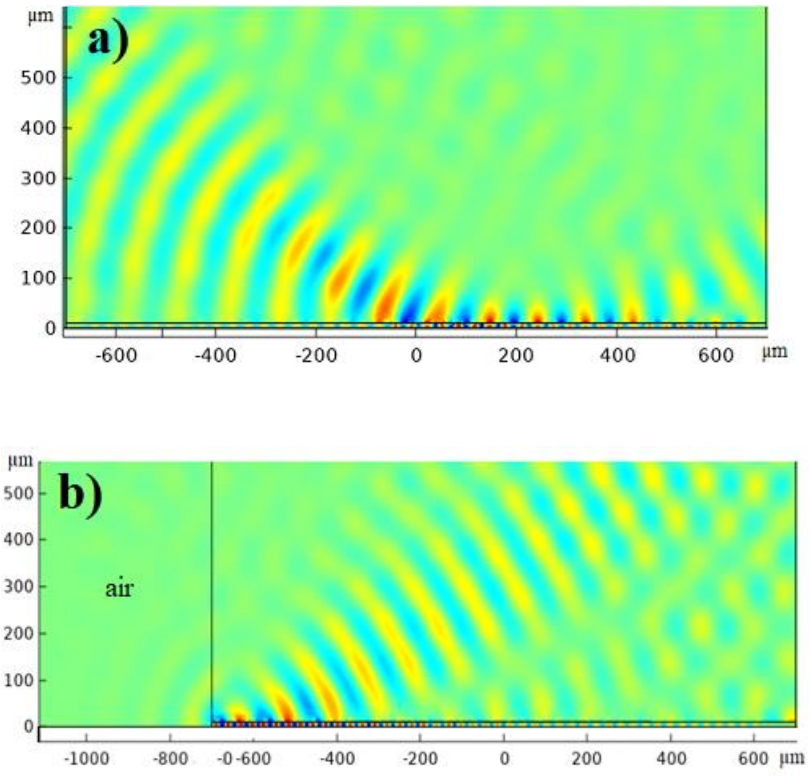

Fig 5. The effect chirped grating on the orientation of laser output intensity when a) the grating period increases as $\Lambda_t = \Lambda_{t-1} + 1$ along the cavity length; and b) when the thickness of grating is initially increases from the left end to the center as $T_t = T_{t-1} + 0.5$ and then from the center to the right end as $T_t = T_{t-1} - 0.5$.

Fig. 5 shows the effect of thickness and grating period on the orientation of laser output intensity. In Fig. 5 (a), we increase the chirped grating period with the criterion $\Lambda_t = \Lambda_{t-1} + 1$, along the longitudinal length of the cavity, so that t is the number of the grating gap. The width of the metal grating and the initial grating period is 20µm and 21µm, respectively. The propagation is tilted with an angle of 45 degrees to the left (negative tilted) and the intensity height is approximately 330µm at a frequency of 2.97THz but is increased the amount of loss (30.31cm^{-1}). In Fig. 5 (b), we have changed the chirped thickness of grating, along the length of the cavity and to the longitudinal center of the cavity according to the criterion $T_t = T_{t-1} + 0.5$ and from the center to the end of the cavity according to the criterion $T_t = T_{t-1} - 0.5$. Λ=38.36µm, initial thickness (T) of the grating is 0.25µm, width of the gap is approximately 0.13Λ. The propagation is tilted with an angle of 45 degrees to the right (positive tilted) and the intensity height is approximately 400µm at a frequency of 2.98 THz but is increased the amount of frequency loss (32.78cm^{-1}) like part (a). In both cases, the width of the absorbing boundaries is 40µm.

Fig. 6 shows the simulated spectra of THz QCLs with antenna-feedback non-chirped and chirped grating schemes. The single-mode spectrum is scaled linearly with a grating period (Λ), indicating that the antenna-feedback

mechanism operates as expected. In addition, the lasing wavelength of the chirped grating is longer than that of the non-chirped one.

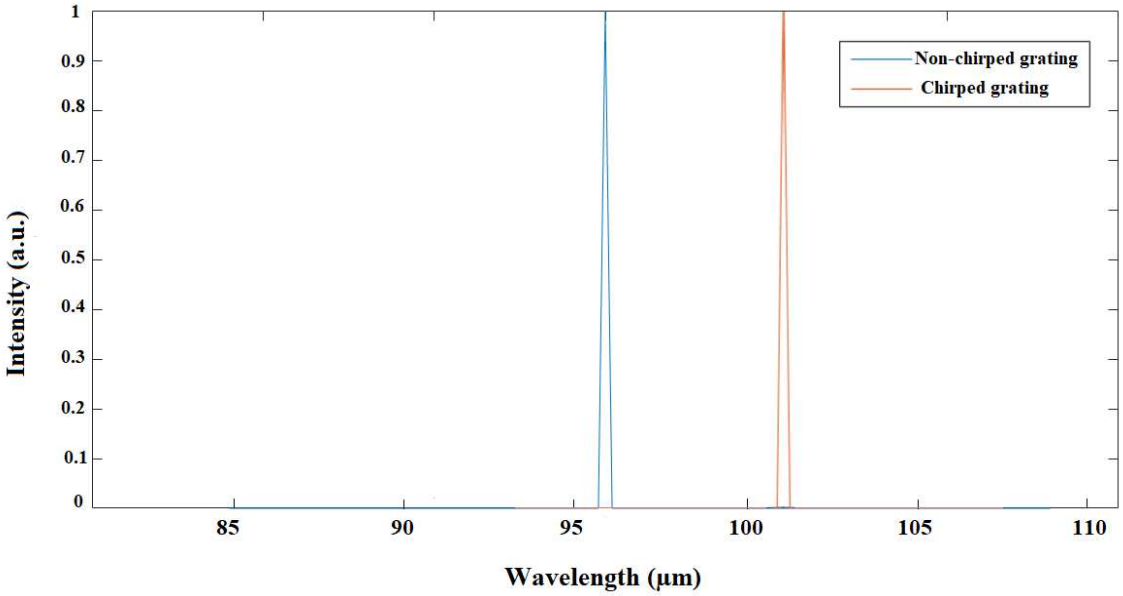

Fig 6. Simulated lasing spectrum for the antenna-feedback THz QCL. The blue line is for the non-chirped grating and the red line for the chirped grating schemes and with the same cavity dimensions.

Table 1. Different parameters used for QCLs simulations [19].

g_0 (1/s)	τ_{31} (ps)	τ_{32} (ps)	τ_{21} (ps)	τ_{sp} (ns)	τ_p (ps)	τ_{out} (ps)	β	M
5.3×10^4	2.4	2.0	0.5	7.0	3.7	0.5	10^{-6}	30

To investigate dynamics characteristics as well as the gain and the output power of the THz QCL, we have numerically solved Eqs. (2-7) together with following Eqs. (8-10) for the parameters listed in Table 1. The injection efficiency is defined as [19]:

$$\eta = \frac{\tau_{31}\left(\tau_{32}-\tau_{21}\right)}{\tau_{32}\left(\tau_{31}+\tau_{21}\right)} \tag{8}$$

where the injection efficiency is obtained as 72% for the parameters given in Table 1.

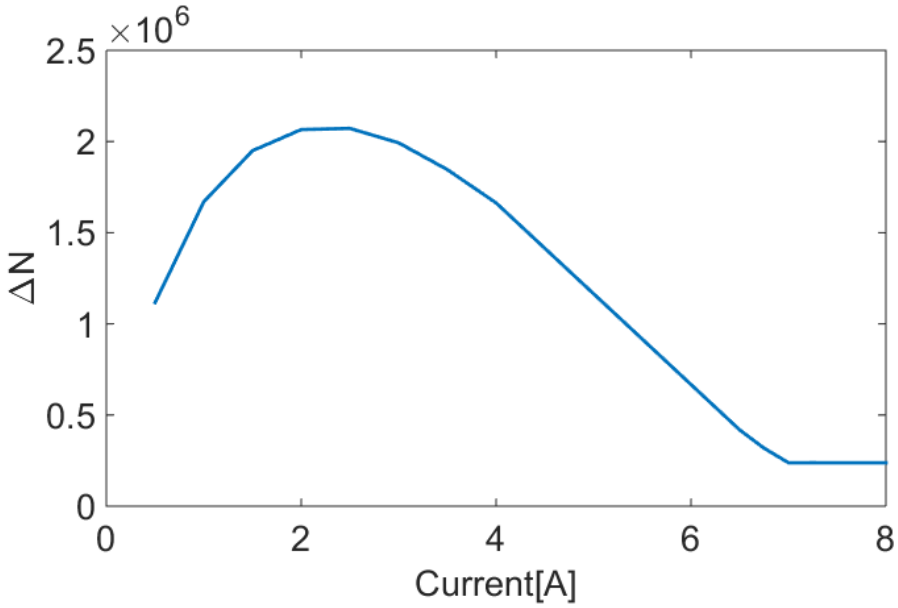

Fig 7. Population inversion as a function of injection current.

As it can be seen from Fig. 7, up to 2.5A electrical injection current, the simulated population inversion increases and then the population inversion decreases. However, it should be noted that in practice, THz QCLs can withstand injection currents up to 4A [20]. It is also possible to plot the dynamics of the carrier population at levels 3 and 2 and the number of cavity photons at different currents. In Fig. 8, evolutions of the carrier populations at levels 3 and 2 together with photon numbers simulated at 2.5A are shown.

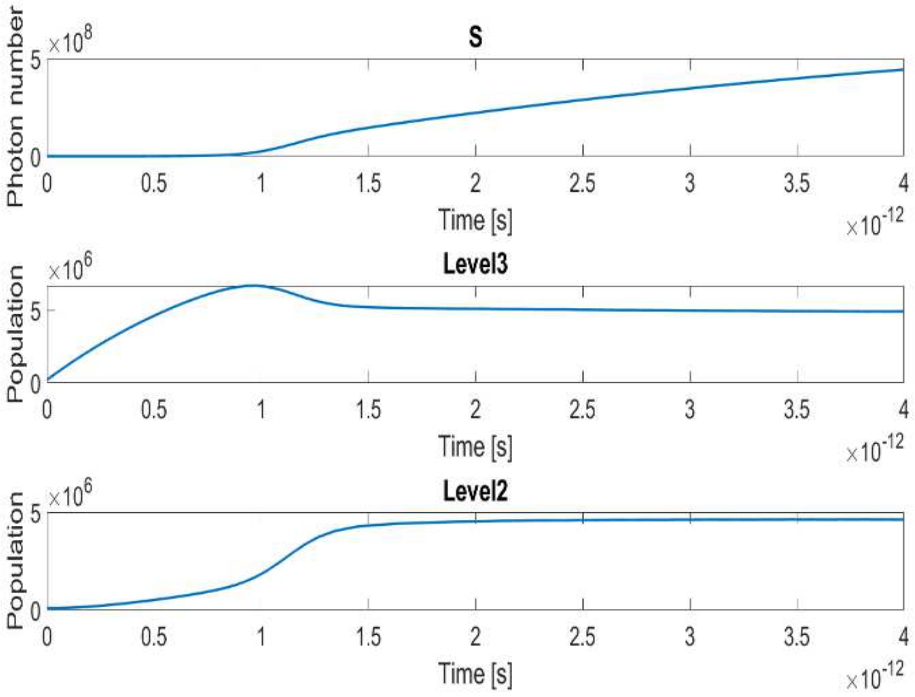

Fig 8. Evolutions of the carrier populations at levels 3, 2 and photon number simulated at 2.5A electrical current.

Using the relationship between the optical output power P and the photons number S given in Eq. (6), the *P-I* diagram is obtained. The mirror loss of the cavity α_{mir} is defined as:

$$\alpha_{mir} = -\frac{1}{2L}\log\left(R_1 R_2\right) \tag{9}$$

where R is the reflection coefficient of the cavity facets.
The *P-I* curve of the THz QCL is shown in Fig. 9 where the solid line corresponds to the non-chirped grating with of Λ =21.7μm, a loss of 12cm^{-1} and the resonance frequency of 3.12THz. Also, the dotted-line is related to the chirped grating with a grating period of $\Lambda_t = \Lambda_{t-1} + 1$, loss of 31.30cm^{-1} and the resonant frequency of 2.97THz, so that t is the number of grating gaps.

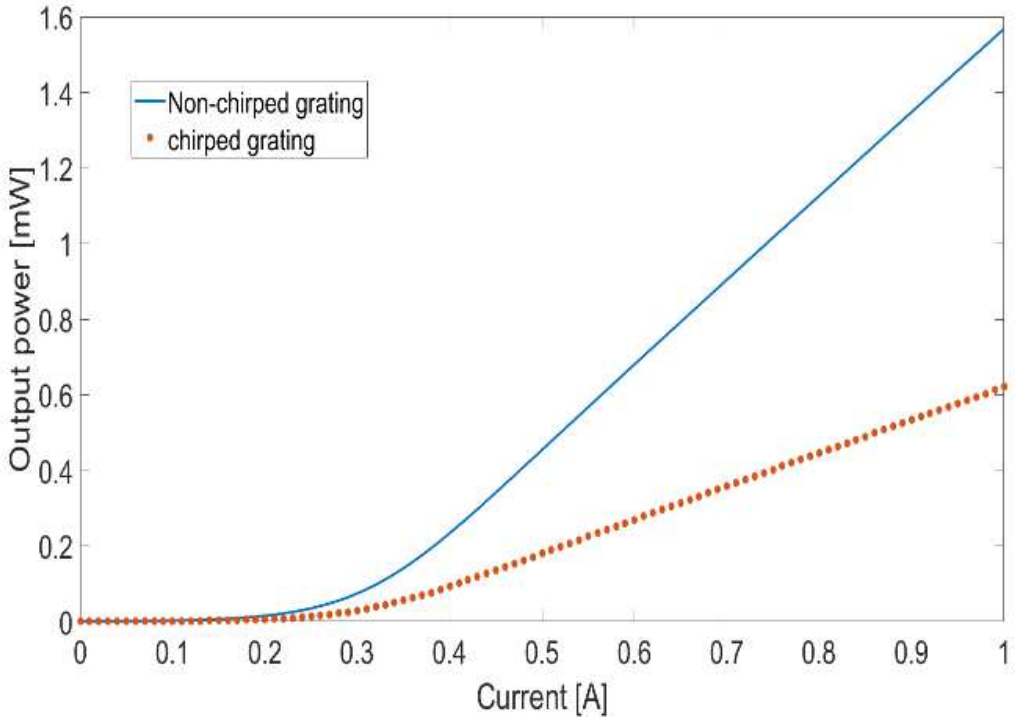

Fig 9. P-I diagram. The blue continuous line diagram is for the non-chirped grating period and the red dotted line diagram is for the chirped grating period.

As is seen in Fig. 9, the output power at 1A electrical current is about 1.5mW for a non-chirped grating period and is about 0.6mW for a chirped grating period. Also, QCLs with the chirped grating have more threshold injection current and lower slope efficiencies than QCLs with the non-chirped grating scheme. This is due to the higher loss caused by the chirped grating.

Optical gain is one of the most important features of semiconductor lasers. Optical gain occurs due to the emission of light created by the recombination of electrons and holes. In other lasers, such as gas lasers or solid-state lasers, the processes involved in the optical operation are very simple, but in semiconductors is a complicated issue due to the interactions between photons, electrons and holes. Accordingly, understanding these processes as an essential requirement for device optimization is necessary. Therefore, we have also examined the optical gain in the three-level THz QCLs. Optical gain is directly related to the population inversion which is obtained using Eq. (7), where $L(f)$ is the Lorentz line shape function defined as follows:

$$L(f)=\frac{\left(\frac{\Delta\upsilon}{2}\right)^2}{(f-f_0)^2+(\Delta\upsilon)^2} \tag{10}$$

Here, Δν is the frequency bandwidth which is equal to 1.5 THz and f_0 is the resonance frequency [21]. Now, using Eq. (7), we can simulate the optical gain spectrum for the three-level THz QCL with the non-chirped or chirped grating scheme as shown in Fig. 10.

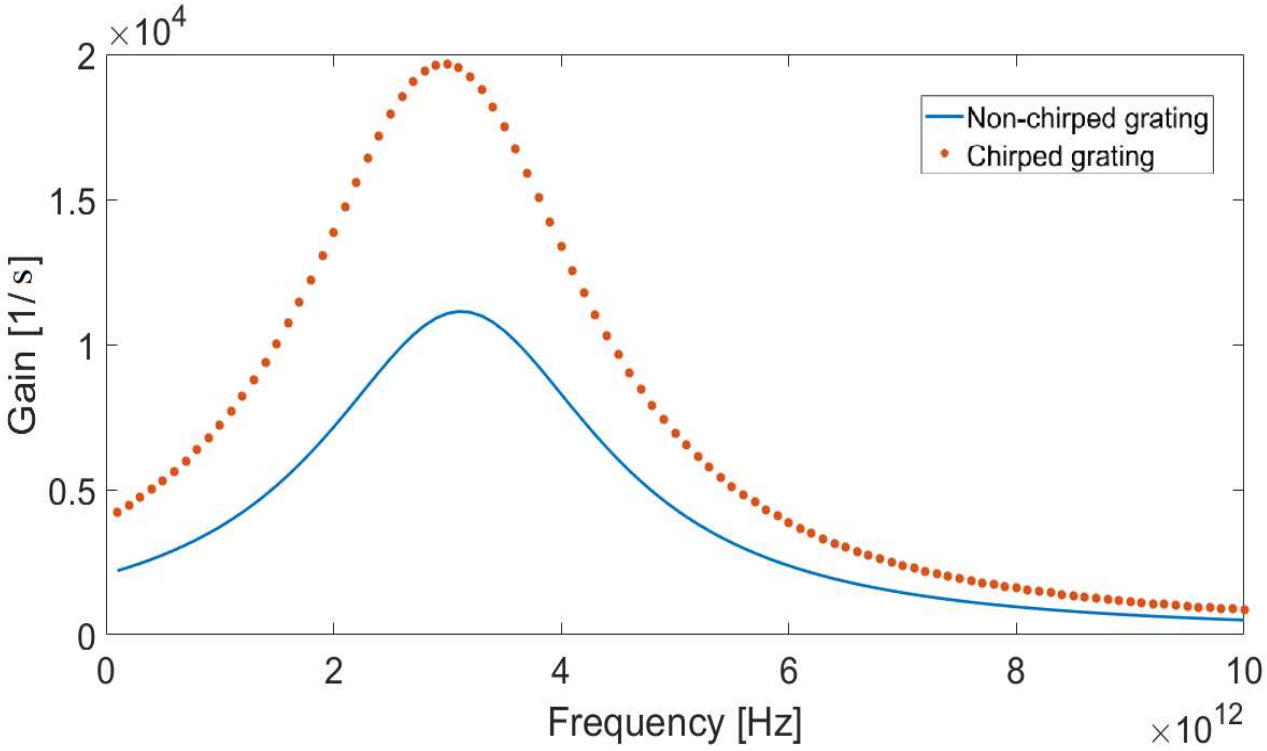

Fig 10. Optical gain spectrum of the THz QCL for the non-chirped grating (solid line) and the chipped grating (dotted line).

As can be seen from Fig. 10, the optical gain value is the order of 10^4 and it obeys the form of Lorentz function which has been also established by other works such as reference [22]. In Fig. 10, the QCL with a non-chirped grating, the value of the optical gain threshold is 0.25×10^4 (s^{-1}) and the gain peak occurs at the resonance frequency of 3.12THz which is approximately equal to 1.1×10^4 (s^{-1}). Also, for the QCL with a chirped grating scheme, the threshold value and the gain peak are higher than those of QCL with a non-chirped grating.

4- Conclusion

We have studied antenna-feedback THz plasmonic QCLs based on the two-dimensional simulation where by changing the thickness of absorbing boundaries at both ends of the cavity, a minimum loss less than 5.9cm^{-1} is achieved. Also, by changing the width and chirped metal grating period, we were able to control the orientation of the output beam vertically or tilted. Tilted propagation has a higher resonant frequency loss and higher intensity than vertical propagation. By solving three-level rate equations, we have simulated the dynamics of the carrier

populations at lasing levels and the number of cavity photons at 2.5A injection current. Finally, using the relationship between the output power and the number of photons, we have plotted the P-I diagram for two types of laser structures with non-chirped and chipped grating schemes with a loss of $12cm^{-1}$ and $30.31cm^{-1}$, respectively. It was observed that THz QCL with chirped grating has a higher threshold current and lower slope efficiency than those of QCL with non-chirped grating due to higher loss .In the optical gain spectrum for QCL with non-chirped grating, the gain threshold is 0.25×10^{4} (s^{-1}) and for the QCL with chirped grating due to further loss, the threshold value is higher than the gain for THz QCL with non-chirped grating.

Funding

No funding was received for this work.

Author contributions

All authors contributed to the study conception and design. Material preparation, simulation results and analysis were performed by H. Pakarzadeh and F. Pakfetrat. The first draft of the manuscript was written by F. Pakfetrat and all authors commented on previous versions of the manuscript. All authors read and approved the final manuscript.

Availability of data and material

Data are available on request from the authors.

Compliance with ethical standards

Compliance with ethical standards is followed by authors.

• Disclosure of potential conflicts of interest

The authors declare that they have no potential conflicts of interests.

• Research involving Human Participants and/or Animals

Not applicable.

• Informed consent

Not applicable.

Consent to participate

Not applicable.

Consent for Publication

Not applicable.

Acknowledgments

Not applicable.

References

[1] Shibuya K., Nawata K., Nakajima Y., Fu Y., Takahashi E. J., Midorikawa K. and Minamide H., "Characteristics of nonlinear terahertz-wave radiation generated by mid-infrared femtosecond pulse laser excitation", *Applied physics express.,* **14.,** 092004-5 (2021).

[2] Tonouchi M., "Cutting-edge terahertz technology", *Nat. Photon.*, **1,** 97–105 (2007).

[3] Williams B. S., " Terahertz quantum cascade lasers", *Nature. Photonics.,* **1**, 517–525 (2007).

[4] Siegel P. H., "THz instruments for space", *IEEE Trans. Antennas Propag.*, **55,** 2957-2965 (2007).

[5] Lewis R. A., "Terahertz imaging and spectroscopy methods and instrumentation", *Elsevier Ltd.,* **1,** 422-426 (2017).

[6] Pawar A. Y., Sonawane D.D., Erande K. B. and Derle D. V., "Terahertz technology and its application", *Drug invention today.,* **5.2,** 157-163 (2013).

[7] Zhang Y., Li K. and Zhao H., "Intense terahertz radiation: generation and application ", *Frontiers of Optoelectronics.,* **14.,** 4-36 (2021).

[8] Kawase K., Sato M., Taniuchi T. and Ito H., "Coherent tunable THz-wave generation from $LiNbO_3$ with monolithic grating coupler", *Appl Phys. Lett.,* **68,** 2483-5 (1996).

[9] Idehara T., Saito T., Ogawa I., Mitsudo S., Tatematsu Y., Agusu L., Mori H. and Kabayashi S., "Development of terahertz FU CW Gyrotron series for DNP", *Appl. Magn. Reson.,* **34,** 265-275 (2008).

[10] Bratman V. L., Kalynov Y. K. and Manuilov V N., "Large-orbit gyrotron operation in the terahertz frequency range", *Phy. Rev. Lett.,* **102,** 245101 (2009).

[11] Kumar V., Varshney R. K. and Kumar S., "Terahertz generation by four-wave mixing and guidance in diatomic teflon photonic crystal fibers", *Optics Communications.,* **1,** 124460-6 (2020).

[12] Chattopadhyay G., "Technology, capabilities, and performance of low power terahertz sources", *IEEE Trans. THz Sci. Technol.,* **1,** 33-53 (2011).

[13] Köhler R. Tredicucci A., Beltram F., Beere H. E., Linfield E. H., Davies A. G., Ritchie D. A., Lotti R. C. and Rossi F., "Terahertz semiconductor-heterostructure laser", *Nature.,* **417,** 156-9 (2002).

[14] Wu C., "Terahertz Plasmonic Lasers with Distributed-Feedback", Lehigh University, Theses and Dissertations., 2882 (2016).

[15] Kumar S., Williams B. S., Qin Q., Lee A.W., Hu Q. and Reno J. L., "Surface-emitting distributed feedback terahertz quantum-cascade lasers in metal-metal waveguides", *Opt. Express.,* **15,** 113-128 (2007).

[16] Amanti M. I., Scalari G., Castellano F., Beck M. and Faist J., "Low divergence terahertz photonic-wire laser", *Opt. Express*., **18,** 6390-6395 (2010).

[17] Gallacher K., Ortolani M., Rew K., Ciano C., Baldassarre L., Virgilio M., Scalari G., Faist J., Gaspare L., Deseta M., Capellini G., Grange T., Birner S. and Pauul J. D., "Design and simulation of losses in Ge/SiGe terahertz quantum cascade laser waveguides", *Opt. Express.,* **28**, 4786-4800 (2020).

[18] Lee S. and Wacker A., "Nonequilibrium Green's function theory for transport and gain properties of quantum cascade structures", *Phys. Rev. B.,* **66,** 245314-18 (2002).

[19] Wang X. G., Grillot F. and Wang C., "Rate equation modeling of the frequency noise and the intrinsic spectral linewidth in quantum cascade lasers", *Opt. express.,* **26,** 002325-002334 (2018).

[20] Yao C., Xu T. H., Wan W. J., Zhu Y. H. and Cao J. C., "An equivalent circuit model for terahertz quantum cascade lasers: Modeling and experiments", *Chin. Phys. B.,* **9,** 094208-4 (2015).

[21] Chan C. W. I., "Towards Room-Temperature Terahertz Quantum Cascade Lasers: Directions and Design", Massachusetts Institute of Technology, PhD Theses and Dissertations., (2015).

[22] Kim J., Lerttamrab M. and Chang S. L., "Theoretical and Experimental Study of Optical Gain and Linewidth Enhancement Factor of Type-I Quantum-Cascade Lasers", *IEEE Journal of quantum electronics,* **40,** 1663-1674 (2004).